BIOLOGY OF REPRODUCTION **81,** 768–776 (2009)
Published online before print 24 June 2009.
DOI 10.1095/biolreprod.109.077909

Evidence That a Defective Spindle Assembly Checkpoint Is Not the Primary Cause of Maternal Age-Associated Aneuploidy in Mouse Eggs[1]

Francesca E. Duncan,[4] Teresa Chiang,[4] Richard M. Schultz,[2] and Michael A. Lampson[3]

Department of Biology, University of Pennsylvania, Philadelphia, Pennsylvania

ABSTRACT

Advanced maternal age is unequivocally associated with increased aneuploidy in human eggs and infertility, but the molecular basis for this phenomenon is unknown. An age-dependent deterioration of the spindle assembly checkpoint (SAC) has been proposed as a probable cause of aneuploidy. Accurate chromosome segregation depends on correct chromosome attachment to spindle microtubules, and the SAC provides time for this process by delaying anaphase onset until all chromosomes are stably attached. If SAC function decreases with age, oocytes from reproductively old mice would enter anaphase of meiosis I (AI) prematurely, leading to chromosome segregation errors and aneuploid eggs. Although intuitively appealing, this hypothesis is largely untested. We used a natural reproductive aging mouse model to determine if a defective SAC is the primary cause of aneuploidy in eggs. We tracked the progress of individual oocytes from young and old mice through meiosis I by time-lapse microscopy and counted chromosomes in the resulting eggs. This data set allowed us to correlate the timing of AI onset with aneuploidy in individual oocytes. We found that oocytes from old mice do not enter AI prematurely compared to young counterparts despite a 4-fold increase in the incidence of aneuploidy. Moreover, we did not observe a correlation between the timing of AI onset and aneuploidy in individual oocytes. When SAC function was challenged with a low concentration of the spindle toxin nocodazole, oocytes from both young and old mice arrested at meiosis I, which is indicative of a functional checkpoint. These findings indicate that a defective SAC is unlikely the primary cause of aneuploidy associated with maternal age.

aging, aneuploidy, meiosis, mouse oocyte, oocyte development, spindle checkpoint

INTRODUCTION

Advanced maternal age is associated with devastating aneuploidies that lead to infertility, fetal loss, or birth defects [1]. The likelihood of a woman in her 40s ovulating an aneuploid egg can be greater than 50% [2], and the probability of her having a trisomic pregnancy is 30%–35%, compared to only 2%–3% in a woman in her 20s [3]. The majority of aneuploidies of maternal origin occur during the first meiotic division [4]. Although several possibilities have been proposed, the molecular defects leading to chromosome segregation errors in meiosis I are unknown [5].

During prophase of meiosis I, homologous chromosomes undergo synapsis and recombination in fetal oocytes. The oocytes then enter a prolonged arrest while residing within primordial follicles; this arrest can last several decades in humans, until oocyte development is initiated and the fully grown oocyte is ovulated between puberty and menopause. When the oocyte resumes meiosis I in response to hormonal cues, homologous chromosomes align at the metaphase plate, establish stable kinetochore-microtubule attachments, and segregate to opposite poles in anaphase of meiosis I (AI). The oocyte then arrests at metaphase of meiosis II (MII) until fertilization.

An age-dependent deterioration of the spindle assembly checkpoint (SAC) in meiosis I has been proposed as a primary cause of aneuploidy in eggs [5, 6]. The SAC is a multi-protein signaling network that delays anaphase onset until all kinetochores are stably attached to spindle microtubules [7]. SAC components, including MAD1, MAD2, BUB1, and BUB1B proteins, localize to unattached kinetochores [8] and generate a diffusible signal to delay anaphase onset by preventing the CDC20-mediated activation of the APC/C, an E3 ubiquitin ligase that targets cyclin B1 and securin for destruction [9]. Without cyclin B1 and securin degradation, cell cycle progression is halted because CDK1 activity remains high and chromosome cohesion is maintained. A weakened SAC would lead to premature anaphase before chromosomes have attached to spindle microtubules, and chromosome segregation errors would inevitably follow.

The SAC has primarily been characterized in mitotic cells, but its function is similar in meiosis in oocytes. For example, oocytes treated with spindle toxins during meiotic maturation arrest at metaphase of meiosis I (MI) presumably because correct kinetochore-microtubule attachments have not been made [10, 11]. Strongly disrupting the SAC, for example by depletion of MAD2, results in a precocious MI-AI transition following germinal vesicle breakdown (GVBD) because the oocytes do not delay AI onset until all kinetochores have attached to spindle microtubules [10, 12–14]. This accelerated progression through meiosis I ultimately generates aneuploidy. The SAC in oocytes is essential for regulating the timing of the MI-AI transition but is not required for maintaining the physiological arrest that occurs at MII [15, 16]. Thus, an age-dependent deterioration of SAC function is a compelling hypothesis to account for maternal age-associated aneuploidy, especially since errors occur more frequently at meiosis I [4].

The idea that the SAC is compromised in oocytes with increased maternal age has been investigated in the senescence-accelerated mouse (SAM), a mouse strain developed as an aging

[1]Supported by a grant from the National Institutes of Health (NIH) (HD058730 to R.M.S. and M.A.L.) and a Bingham Trust award from the Institute of Aging at the University of Pennsylvania. F.E.D. was supported by a training grant from the NIH (T32 HD 007305 22).
[2]Correspondence: Richard M. Schultz, Department of Biology, University of Pennsylvania, 433 S. University Ave., Philadelphia, PA 19104. FAX: 215 898 8780; e-mail: rschultz@sas.upenn.edu
[3]Correspondence: Michael A. Lampson, Department of Biology, University of Pennsylvania, 433 S. University Ave., Philadelphia, PA 19104. FAX: 215 898 8780; e-mail: lampson@sas.upenn.edu
[4]These authors contributed equally to this work.

Received: 31 March 2009.
First decision: 5 May 2009.
Accepted: 14 June 2009.

eISSN: 1259-7268 http://www.biolreprod.org
ISSN: 0006-3363

model that shows an early decline in fertility [17]. During meiotic maturation, many oocytes from 10- to 14-month-old SAM mice progress prematurely to MII despite having disrupted MI spindles and chromosome misalignment, suggesting a defective SAC [18]. The SAM mouse may not be a suitable reproductive aging model, however, because the observed meiotic errors are much more frequent and severe than what occurs in a naturally aging population [19]. Furthermore, the SAM phenotype is due to mitochondrial dysfunction and oxidative damage [20, 21], but it is not known whether these events actually cause meiotic defects during natural aging.

The most physiologically relevant method to determine if a defective SAC contributes to the maternal age-associated increase in aneuploidy is to simply study reproductively old animals. Mice that are 60–70 wk old, corresponding to women ages 38–45 based on a linear extrapolation estimate, ovulate fewer eggs and have a higher incidence of aneuploid eggs compared to 6- to 8-wk-old mice [19]. Gene expression profiling studies in this model system showed that transcripts encoding several key components of the SAC, including BUB1 and CDC20, were misexpressed in old oocytes, suggesting that the SAC may be perturbed [19].

Misexpression of SAC components likely varies among oocytes, which could explain why only a fraction of old eggs are aneuploid. If a defective SAC is in fact a primary cause of the maternal age-associated increase in aneuploidy, we would make two predictions in our natural aging mouse model. First, if the checkpoint does not effectively delay AI onset, old oocytes would progress more rapidly through meiosis I compared to young oocytes. Second, those oocytes that enter AI earlier are more likely to become aneuploid. To test these predictions, we followed individual oocytes through meiosis I by time-lapse microscopy and subsequently counted chromosomes in the same MII-arrested egg to assess aneuploidy. We were thus able to correlate the duration of meiosis I with the chromosome count for each individual egg. Moreover, because we tracked oocytes from individual mice separately, we were able to examine animal-to-animal variability. We find that the timing of meiotic progression is similar in young and old oocytes and does not correlate with aneuploidy. Furthermore, when SAC function was challenged by exposure to a low concentration of the spindle toxin nocodazole, both young and old oocytes arrested in meiosis I. Our results indicate that the SAC is functional in young and old oocytes and is likely not the primary defect leading to the maternal age-associated increase in aneuploidy.

MATERIALS AND METHODS

Oocyte Collection and Culture

Young B6D2F1/J (6–14 wk) female mice and old B6D2F1 female mice (16–19 mo) were obtained from The Jackson Laboratory (Bar Harbor, ME) and National Institutes of Aging (Bethesda, MD), respectively. Fully grown, germinal vesicle (GV)-intact oocytes from gonadotropin-treated females were collected in modified Hepes-buffered Whitten medium [22] and cultured in CZB medium [23] as previously described [24]. All culture was done at 37°C in a humidified atmosphere of 5% CO_2 in air. When applicable, the medium was supplemented with 2.5 μM milrinone, an oocyte-specific PDE3 inhibitor that reversibly prevents spontaneous resumption of meiosis [25]. All animal experiments were approved by the Institutional Animal Use and Care Committee and were consistent with National Institutes of Health guidelines.

Time-Lapse Microscopy of Meiotic Progression

To initiate meiotic maturation, oocytes from a single young or a single old mouse were washed through three drops of CZB to remove the milrinone, and each individual oocyte was then transferred to a 3-μl drop of CZB in a FluoroDish (World Precision Instruments, Inc., Sarasota, FL). The oocytes were imaged by time-lapse microscopy beginning 1 h after milrinone washout. Images were acquired on a Leica DMI4000B (Leica Microsystems, Inc., Wetzlar, Germany) inverted microscope equipped with a 100× 1.4 NA objective, differential interference contrast (DIC) optics, and a cooled CCD camera (Retiga-EXi; QImaging, BC, Canada). A computer-driven, motorized X-Y-Z stage (ASI, Eugene, OR) permitted multiple points to be revisited over time so that multiple oocytes could be imaged in parallel. IPLab software (BD Biosciences, Rockville, MD) was used for image acquisition. A constant temperature of 37°C and an atmosphere of 5% CO_2 were maintained with an environmental chamber, a heated stage insert, and a CO_2 controller (PeCon, Erbach, Germany). Oocytes were imaged by DIC every 30 min for 8.5 h and then every 15 min for another 3.5 h, for a total of 12 h after milrinone washout. Images were analyzed using ImageJ software (National Institutes of Health, Bethesda, MD).

Monastrol Treatment, Kinetochore Immunocytochemistry, and Chromosome Counting

To determine the chromosome count following time-lapse microscopy, eggs were cultured for 1 h in CZB containing 100 μM monastrol (Sigma, St. Louis, MO), a kinesin-5 inhibitor. This treatment causes the bipolar MII spindle to collapse into a monopolar spindle and results in the dispersion of chromosomes [26]. Eggs were fixed in freshly prepared 2% paraformaldehyde in PBS for 20 min, permeabilized in PBS containing 0.3% bovine serum albumin (BSA) and 0.1% Triton X-100 for 15 min, and blocked in PBS containing 0.3% BSA and 0.01% Tween-20 (blocking solution). Cells were incubated in a 1:40 dilution of human CREST autoimmune serum (Immunovision, Springdale, AZ) for 1 h followed by washes in blocking solution. The primary antibody was detected using an Alexa-Fluor 594-conjugated goat anti-human secondary antibody (Invitrogen, Carlsbad, CA). Cells were washed in blocking solution, incubated in a 1:5000 dilution of Sytox Green nucleic acid stain (Invitrogen) for 10 min, and mounted in Vectashield (Vector Laboratories, Burlingame, CA).

Images were collected at 0.4-μm intervals to span the entire region of the MII spindle (16–20 μm total) using the microscope described above with a Yokogawa spinning disk confocal and an electron multiplier CCD camera (C9100–13, Hamamatsu, Japan) and processed using ImageJ software. To obtain a chromosome count for each egg, serial confocal sections were analyzed to determine the total number of kinetochores. Sister kinetochores, typically found within 0.8 μm of each other, were assigned by proximity to a specific sister chromatid pair. In cases where it was difficult to distinguish between closely positioned sister kinetochores and a single kinetochore, single sections covering the kinetochore(s) were merged in pseudocolor to see if spectral separation was observed (Supplemental Fig. S1, available online at www.biolreprod.org). The presence of distinct colors indicated a shift in the fluorescent signal, which would only be detected if there were two kinetochores. A single color indicated only one kinetochore center. Two individuals (F.E.D. and T.C.) determined chromosome counts independently, and eggs with ambiguous counts were excluded from the final aneuploidy determination.

AI Imaging Experiments Using H2B-GFP

To determine the precise timing of AI onset relative to polar body emission (PBE) timing, chromosome movements were visualized by microinjecting oocytes with cRNA encoding GFP-tagged H2B. The coding sequence of *H2b* fused to *Gfp* was engineered to contain an N-terminal abbreviated Kozak sequence [27]. The resulting cDNA was subcloned into the pIVT vector [28] using unique *Sal*I and *Sma*I sites. Complementary RNA was synthesized from linearized plasmid DNA using the T7 mMESSAGE mMACHINE kit (Ambion, Austin, TX) according to the manufacturer's instructions. The cRNA was purified using the Qiagen RNeasy Mini kit (Qiagen, Valencia, CA) according to the manufacturer's instructions, and the final cRNA concentration and integrity were determined by spectrophotometry and electrophoresis on a formaldehyde gel, respectively. Approximately 5–7 pl of cRNA (10 ng/μl) was microinjected into the cytoplasm of GV-intact oocytes using a Harvard Apparatus PLI-100 Pico-Injector (Harvard Apparatus, Holliston, MA) on the stage of a Nikon Eclipse TE2000 microscope (Nikon Instruments Inc., Melville, NY) equipped with Hoffman optics and motorized Eppendorf micromanipulators.

To monitor AI, we used an automated method to dilute the milrinone to a concentration that allowed resumption of meiosis at a specified time. Following microinjection, oocytes were cultured in CZB containing 2.5 μM milrinone for approximately 4 h to allow for protein expression and then transferred to a 200-μl drop of CZB containing 0.75 μM milrinone for 8–10 h. This is the minimum milrinone concentration necessary to maintain meiotic arrest, and when the milrinone was diluted to 0.01 μM by timed CZB infusion (Model R-E Syringe Infusion Pump; Razel Scientific Instruments, St. Albans, VT), oocytes resumed

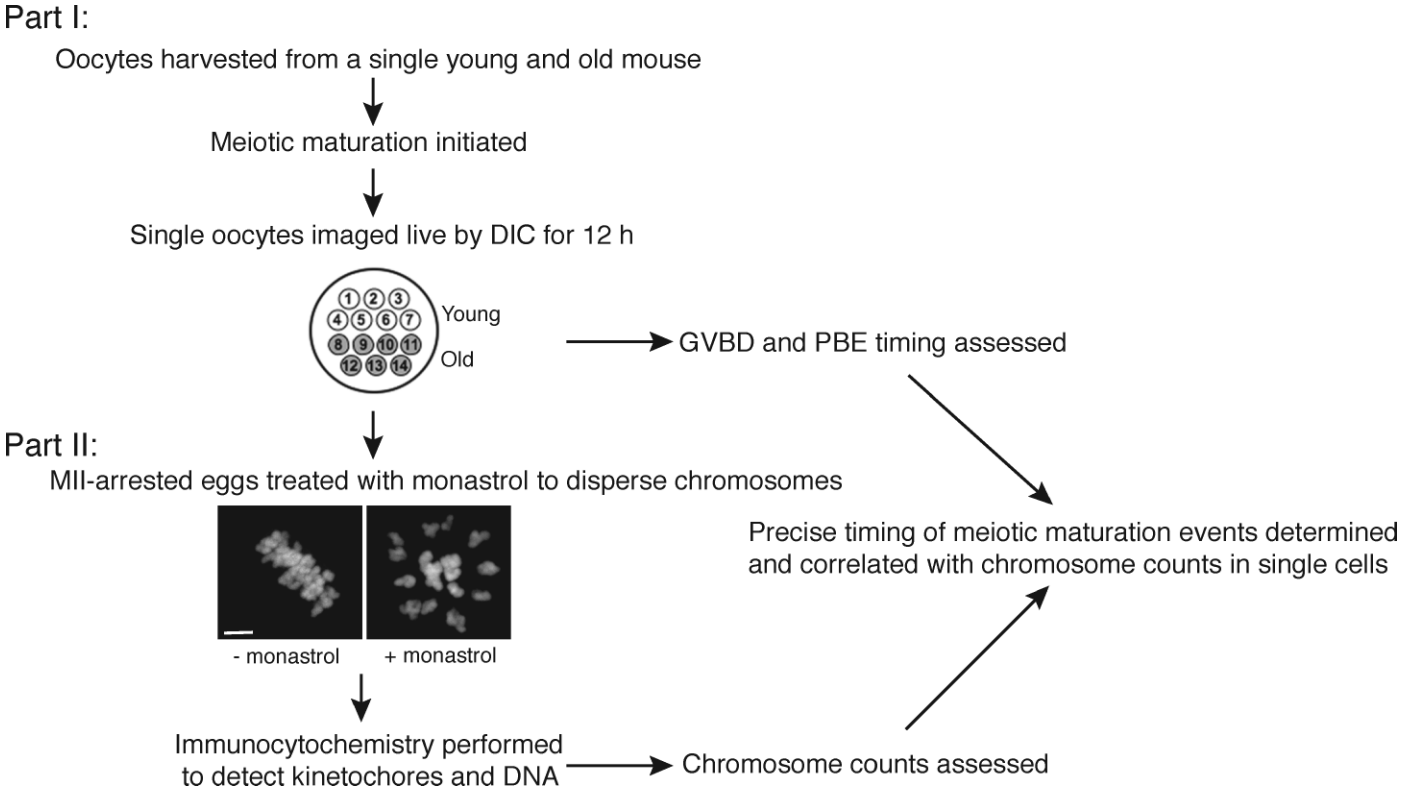

FIG. 1. Experimental design for comparing meiotic progression and aneuploidy in individual young and old oocytes. Meiotic progression was monitored by time-lapse microscopy for 14 oocytes (seven young and seven old) in parallel (Part I). After live imaging, oocytes were cultured for 1 h in monastrol then fixed and processed for immunocytochemistry to label chromosomes and kinetochores (Part II). Chromosomes were counted to assess aneuploidy in each MII-arrested egg. The image shows that 1-h culture with monastrol effectively disperses the MII chromosomes, visualized by Sytox. Bar = 5 μm.

meiosis and reached MII with normal kinetics and proper chromosome alignment. To monitor AI by live imaging, oocytes were transferred to individual 3-μl drops of CZB in a FluoroDish 7-h postmilrinone dilution. DIC images were collected as described above every 5 min until AI onset as assessed by the initial separation of chromosomes. At AI onset, the oocytes were imaged by DIC and fluorescence every 2 min until the completion of chromosome separation. At each time point a *z* series of 11 images was collected at 3-μm intervals. The spinning disk confocal described above was used for fluorescence imaging.

Nocodazole Treatment of Oocytes

To induce an MI arrest, oocytes from young and old mice were collected and matured in the continuous presence of CZB containing 0.04 μg/ml nocodazole in dimethyl sulfoxide (DMSO; Sigma) as previously described [29]. As a control, oocytes were incubated in the same dilution of DMSO alone. Oocytes were imaged by bright field using a 20× objective every 30 min and scored for PBE. At 13–14 h after meiotic resumption, nocodazole was removed, the ability of the cells to progress to MII was assessed, and the chromosome counts of the resulting eggs were determined.

Statistical Analysis

A chi-square test with Yates' correction, an unpaired Student *t*-test, or a two-way ANOVA analysis was performed, as indicated in *Results* or the figure legends, using Prism (GraphPad Software, Inc., San Diego, CA) to evaluate the statistical significance of the differences we observed between young and old oocytes. Differences of $P < 0.05$ were considered to be significant.

RESULTS

Meiotic Progression and Chromosome Count Can Be Assessed in Individual Oocytes

We developed a two-part experimental approach to correlate the timing of meiotic maturation with aneuploidy in single oocytes from young and old mice (Fig. 1). First, oocytes from individual young and old mice were harvested, the onset of meiotic maturation was synchronized by removal of milrinone from the culture medium, and oocytes were imaged individually by time-lapse DIC microscopy until 12 h after maturation onset (Figs. 1 and 2A). For each oocyte, the images were analyzed to determine the timing of GVBD and PBE as determined by the disappearance of the nuclear envelope and complete cytokinesis between the egg and polar body (PB), respectively (Fig. 2A). The duration of meiosis I, defined as the time difference between GVBD and PBE, was also determined for each oocyte because this represents the critical time frame during which the cell assembles a bipolar spindle, aligns its chromosomes on the MI plate, and establishes proper kinetochore-microtubule attachments.

We chose to use PBE as a morphological marker for SAC satisfaction instead of AI onset because PBE is easily scored by minimally perturbing DIC imaging. Furthermore, the timing of these two events is tightly coupled. In oocytes where AI onset could be observed clearly by DIC alone, AI onset and PBE were separated by 0.70 ± 0.06 h and 0.74 ± 0.08 h in young and old oocytes, respectively (Fig. 2, B and C). When chromosome movements were visualized by microinjecting oocytes with cRNA encoding GFP-tagged H2B, we confirmed that AI onset preceded PBE by approximately 0.75 h (Fig. 2D).

In the second part of our experimental approach, we developed a method to accurately count chromosomes in the resulting eggs (Figs. 1 and 3). Following imaging, monastrol-treated eggs were fixed, and kinetochores and chromosomes were visualized by immunocytochemistry (Fig. 3, A and C). Kinetochores, of which there are 40 in a euploid mouse egg, were counted by analyzing serial confocal sections that

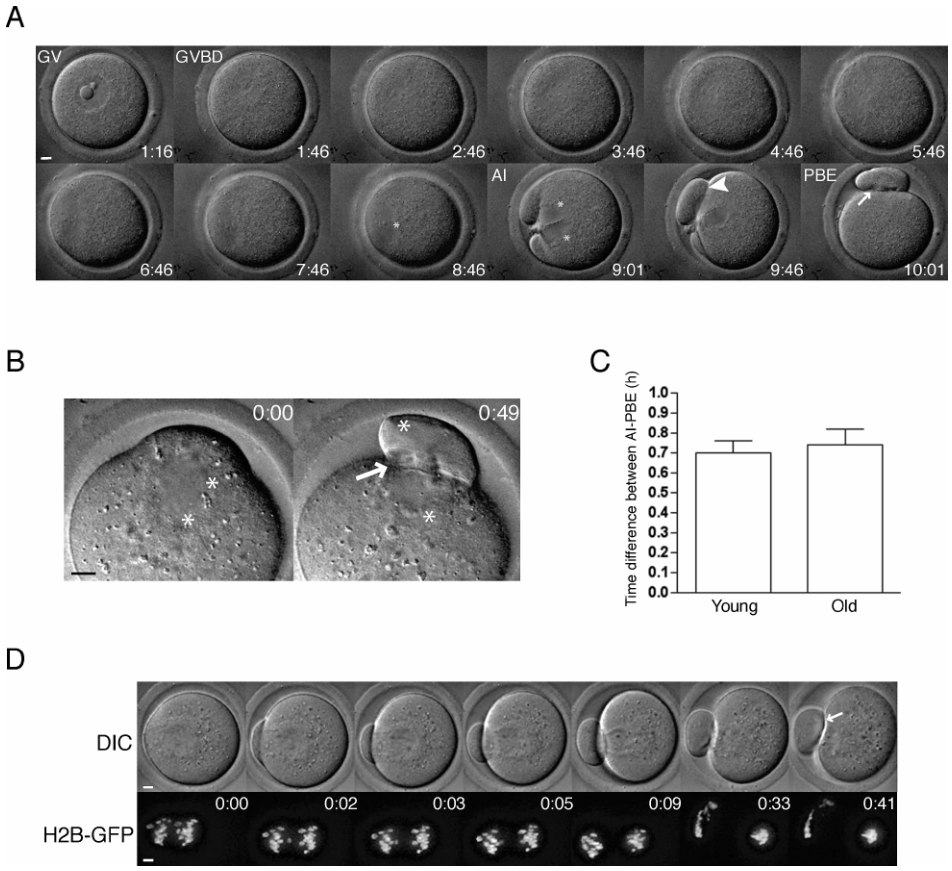

FIG. 2. Tracking meiotic progression by time-lapse microscopy. **A**) A representative series of DIC images shows meiotic progression in an individual oocyte. **B**) AI was monitored in oocytes where the chromosomes were clearly visible by DIC, and a representative series is shown. **C**) The average time of AI onset to complete PBE in young and old oocytes was assessed by analysis of DIC images. Data are shown as mean ± SEM (n = 21 young and 15 old oocytes). The timing of AI onset and PBE were tightly coupled, and there was no statistically significant difference between young and old oocytes (unpaired *t*-test; $P = 0.6439$). **D**) Chromosome movement in young and old oocytes microinjected with *H2b-Gfp* cRNA was visualized during AI using time-lapse confocal microscopy. Upper panels show DIC images, and lower panels show H2B-GFP fluorescence. A total of 11 young and 14 old oocytes were imaged, and a set of representative images is shown. Asterisks mark the position of chromosomes in all images, the arrowhead shows incomplete cytokinesis between the egg and the PB, and the arrow highlights complete membrane separation. Time stamps (h:mm) in **A** label time following removal of milrinone from the culture medium and in **B** and **D** label elapsed time from AI onset as indicated by initial chromosome separation. Bar = 5 μm.

spanned the entire region of the spindle. In this technique, chromosome loss does not occur, because the eggs are maintained in an intact state. Thus, we reliably counted 40 kinetochores in euploid eggs and also accurately detected both hyperploidy and hypoploidy (Fig. 3, B and D). This method is advantageous over more traditional chromosome-spreading techniques that require dissolution of the cell and can only be used to assess hyperploidy because of potential chromosome loss inherent in the procedure [30, 31].

The Timing of Meiotic Progression Is Similar Between Young and Old Oocytes

To monitor meiotic progression, we isolated oocytes from antral follicles and obtained an average of 11 oocytes per old mouse (n = 8) compared to 51 oocytes per young mouse (n = 8). This result is consistent with the age-dependent decline in the number of eggs ovulated in this strain [19]. Following removal of milrinone from the medium, 98% (n = 55) of young

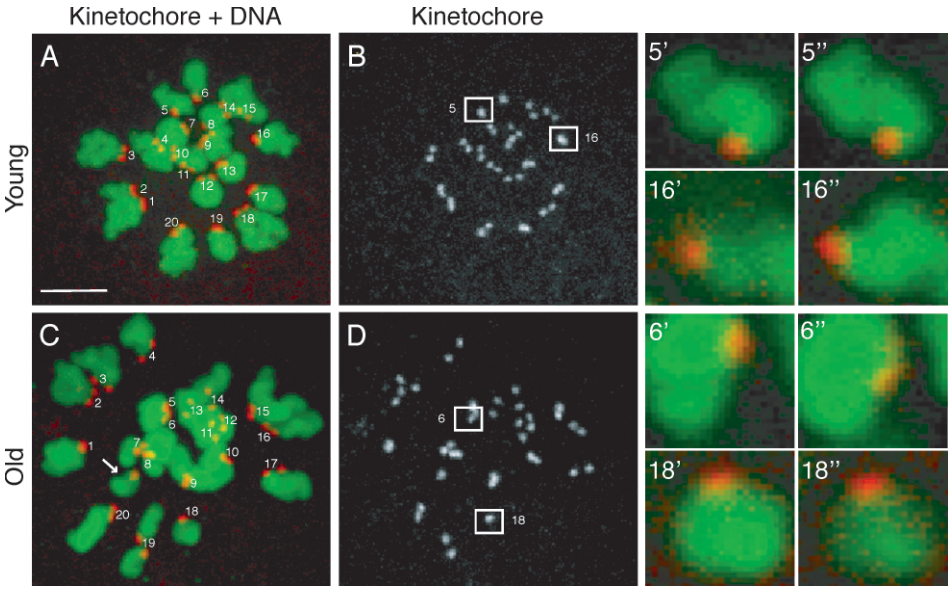

FIG. 3. Determining chromosome number in intact eggs. **A–D**) To count chromosomes following live imaging, eggs were treated with monastrol, then fixed and stained for kinetochores using human CREST autoimmune antiserum (grayscale or red) and for chromosomes using Sytox (green). Representative projected images from young (**A**, **B**) and old (**C**, **D**) eggs are shown. In the merged image of kinetochores and DNA (**A** and **C**), sister kinetochore pairs are labeled from 1–20. The arrow highlights a single extra chromatid in the old egg (**C**), indicating hyperploidy. Boxed kinetochore pairs in **B** and **D** are magnified (right) to show distinct kinetochores at different *z* planes (' and "). The kinetochores in pairs 5' and 5" and in 6' and 6" are separated by 0.8 μm in the *z* direction; the kinetochores in pairs 16' and 16" and in 18' and 18" are separated by 1.2 μm. Bar = 5 μm.

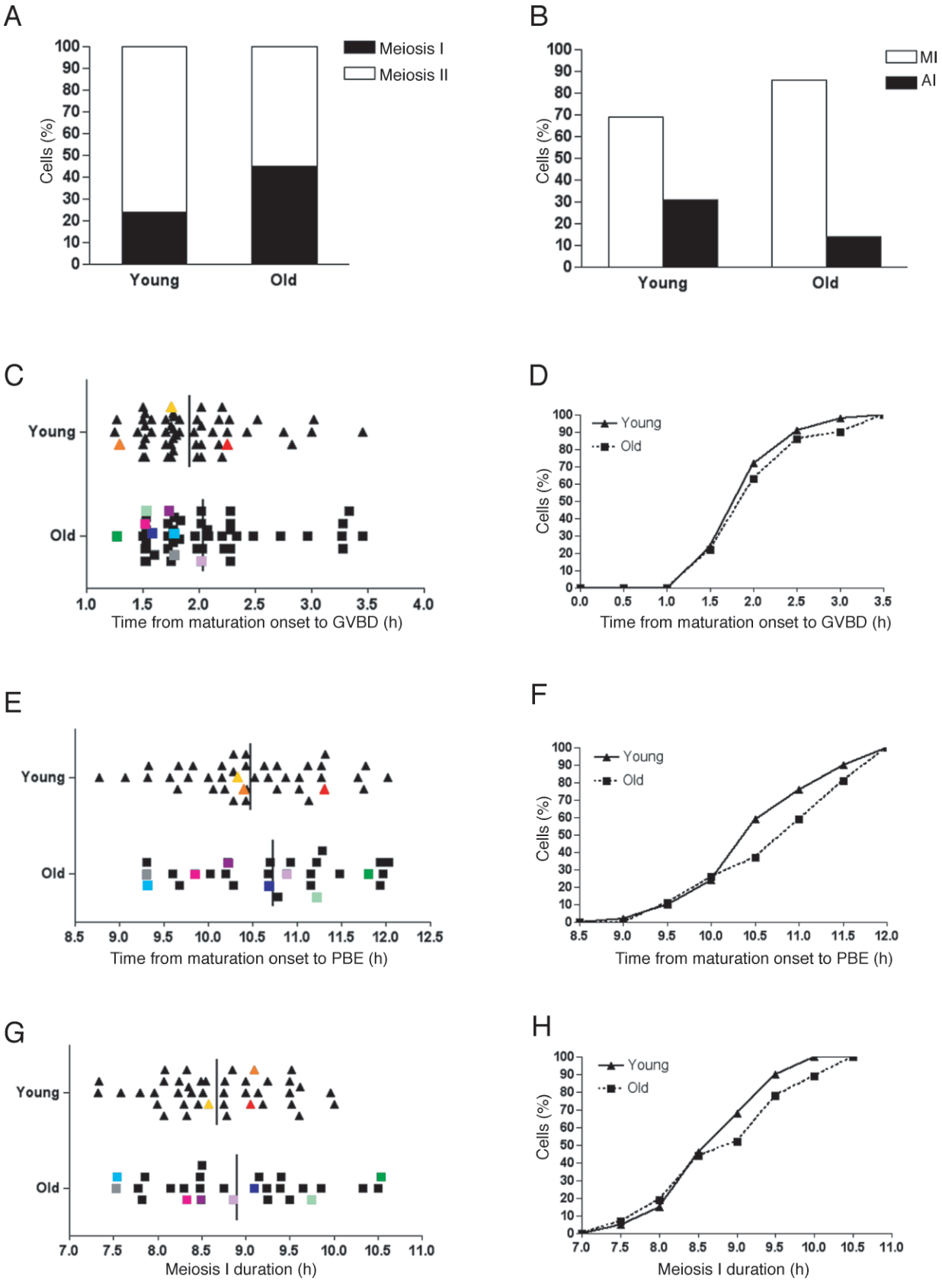

FIG. 4. Timing of meiotic maturation and incidence of aneuploidy in young and old oocytes. **A**) Following time-lapse microscopy to track meiotic progression in individual oocytes, DIC images were analyzed to score the percent of young and old oocytes that reached meiosis II or remained in meiosis I 12 h after milrinone removal. **B**) Oocytes that were still in meiosis I by 12 h were characterized as being either in MI (chromosomes aligned) or AI (chromosomes separated). **C**–**H**) For each oocyte that reached MII in 12 h, the timing of GVBD (**C**, **D**) and PBE (**E**, **F**) was determined, and MII chromosomes were counted. Meiosis I duration was calculated as the time between GVBD and PBE (**G**, **H**). Data are shown for individual oocytes in **C**, **E**, and **G**. Each triangle corresponds to a single young oocyte and each square to an old oocyte. Each color represents a single oocyte tracked through meiotic

TABLE 1. Meiotic progression and aneuploidy in young and old oocytes.

Parameter	Young	Old	Statistics
Total no. of mice used	8	8	
Average no. of oocytes collected/mouse	51	11	Unpaired *t*-test, $P < 0.0001$
Total no. of oocytes imaged	55	52	
No. of GVBD/total imaged (%)	54/55 (98%)	49/52 (94%)	$\chi^2 = 0.321$, $P = 0.5707$
No. of meiosis I/total GVBD (%)	13/54 (24%)	22/49 (45%)	$\chi^2 = 0.620$, $P = 0.4312$
No. of MI oocytes/total MI (%)	9/13 (69%)	19/22 (86%)	
No. of AI oocytes/total MI (%)	4/13 (31%)	3/22 (14%)	
No. of PBE/total GVBD (%)	41/54 (76%)	27/49 (55%)	$\chi^2 = 4.082$, $P = 0.0434$
No. of eggs counted/total no. PBE (%)	37/41 (90%)	23/27 (85%)	
No. of aneuploid eggs/total no. of eggs counted (%)	3/37 (8%)	8/23 (35%)	$\chi^2 = 5.077$, $P = 0.0243$
No. of hyperploid eggs/total no. of aneuploid eggs (%)	1/3 (33%)	5/8 (62%)	
No. of hypoploid eggs/total no. of aneuploid eggs (%)	2/3 (67%)	3/8 (38%)	

and 94% (n = 52) of old oocytes resumed meiosis (Table 1). Of the cells that resumed meiosis, 76% of the young oocytes emitted a PB and reached MII in the 12-h period compared to only 55% of old oocytes (Fig. 4A and Table 1; $\chi^2 = 4.082$, two-tailed $P = 0.0434$). The oocytes that remained in meiosis I were further categorized as either being in MI or AI depending on their chromosome configuration. Although a greater fraction of young oocytes progressed further in the cell cycle (Fig. 4B), this difference was not statistically significant.

We monitored the timing of GVBD in all oocytes and of PBE in those that reached MII during the 12-h period of our experiment. The distribution of GVBD timing, when examined on a single oocyte basis, was similar in young and old oocytes (Fig. 4C). On average, GVBD occurred at 1.92 ± 0.06 h after maturation onset in young oocytes compared to 2.04 ± 0.08 h in old oocytes (Fig. 4C; unpaired *t*-test, $P = 0.2351$). The kinetics of young and old oocytes having undergone GVBD was similar (Fig. 4D). The average timing of PBE after resumption of meiosis was also similar between the two groups of oocytes: 10.48 ± 0.11 h in young oocytes and 10.72 ± 0.19 h in old oocytes (Fig. 4E; unpaired *t*-test, $P = 0.2238$).

When the same data were presented as a cumulative percentage, the timing of PBE was comparable in young and old oocytes that emitted a PB (Fig. 4F). Given that, overall, both GVBD and PBE timing were similar between young and old oocytes, it was not surprising that the duration of meiosis I also was not statistically different (Fig. 4, G and H; unpaired *t*-test, $P = 0.2277$). In young oocytes, meiosis I lasted 8.68 ± 0.10 h after maturation onset compared to 8.91 ± 0.19 h in old oocytes, not including those oocytes that failed to progress to MII during the 12-h period. Together these data demonstrate that old oocytes do not enter AI earlier than young counterparts. Instead, old oocytes on average had a longer meiosis I duration or failed to progress to MII during the time examined compared to young oocytes.

Aneuploidy in Eggs Does Not Correlate with Meiosis I Duration

One strength of our experimental approach is that we obtained accurate chromosome counts for greater than 85% of the eggs following time-lapse imaging, and we superimposed this information on each egg's meiotic maturation history (Table 1). We were thus able to determine if the duration of meiosis I predicts aneuploidy. When we analyzed the data from our eight experimental replicates together, overall aneuploidy was observed in 8% (n = 37) of young eggs compared to 35% of old eggs (n = 23; Fig. 4, C, E, and G, and Table 1). Hyperploidy, consisting of a gain of either a single sister chromatid or a chromatid pair, accounted for one of three young and five of eight old aneuploid eggs. Hypoploidy, consisting of a loss of either a single sister chromatid or a chromatid pair, accounted for the remaining aneuploid eggs. We found that both young and old aneuploid eggs appeared to be randomly distributed with respect to the duration of meiosis I (Fig. 4G). These results indicate that aneuploidy does not correlate with an accelerated AI onset.

We also evaluated our data on an individual mouse basis. Three of eight young mice and five of eight old ones had aneuploid eggs (Fig. 5). These data suggest that aneuploidy is a more general phenomenon in the aging population and cannot be attributed to a specific mouse. We did not observe any obvious differences in the timing of GVBD, PBE, or the duration of meiosis I between individual mice (Fig. 5). These results are consistent with what was observed when the oocytes were analyzed as a cohort (Fig. 4, C, E, and G). Although it does not appear that there is a direct correlation between meiosis I duration and aneuploidy, there does seem to be a trend that oocytes that become aneuploid are among the first to undergo GVBD (Figs. 4C and 5, A and B).

Oocytes from Old Mice Are Able to Mount an MI Arrest in Response to a Low Concentration of Nocodazole

As another test of whether the SAC is equivalently active in young and old oocytes, oocytes were matured in a low concentration (0.04 μg/ml) of the spindle poison nocodazole, which activates the spindle checkpoint and arrests oocytes in MI. This method has been used previously to show that inhibition of BRCA1 overrides the arrest, indicating that BRCA1 is required for normal checkpoint function [29]. If old oocytes have a less robust SAC than young oocytes, we predict that they would arrest less effectively in the presence of a low concentration of nocodazole.

progression that was determined to be aneuploid at MII. Vertical bars mark the average time of each meiotic maturation event, and no statistically significant differences between young and old oocytes were observed. (Unpaired *t*-test, $P = 0.2351$ for GVBD, $P = 0.2238$ for PBE, and $P = 0.2277$ for MI duration). The same data are presented as cumulative percentages in **D**, **F**, and **H**. A chi-square test with Yates correction demonstrated that there was no statistically significant difference at each time point between young and old oocytes ($\chi^2 < 3.84$, two-tailed $P > 0.05$). The data set includes eight experiments with a total of 54 young and 49 old oocytes.

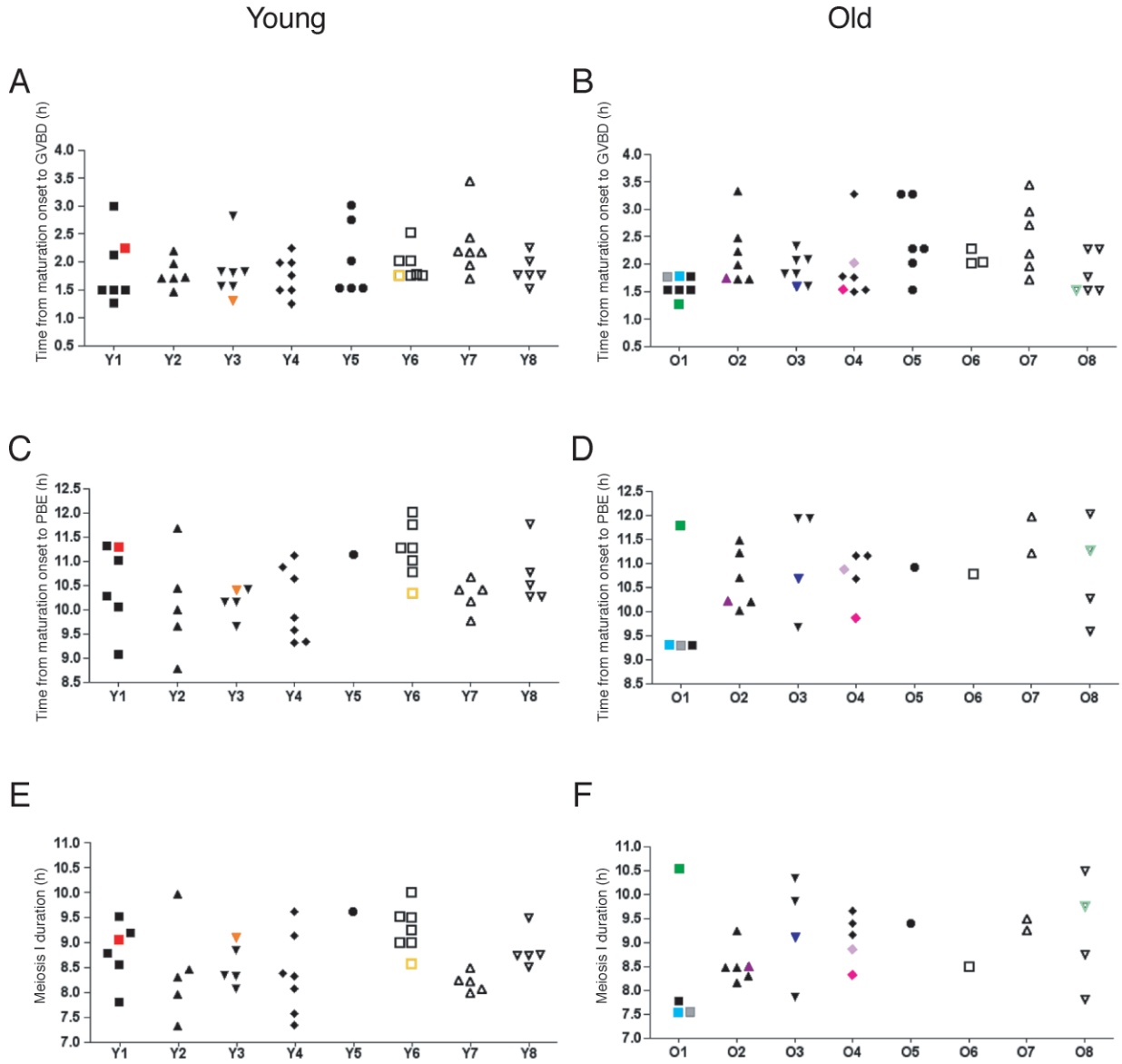

FIG. 5. Meiotic progression and aneuploidy assessed in individual mice. In another representation of the data in Figure 4, the timing of GVBD (**A**, **B**), PBE (**C**, **D**), and meiosis I duration (**E**, **F**) are shown for each oocyte. Oocytes from individual young (**A**, **C**, **E**) and old (**B**, **D**, **F**) mice are grouped and labeled Y1–Y8 (young) and O1–O8 (old). A total of 16 mice (eight young and eight old) were used for these experiments. Each color, consistent with the scheme in Figure 4, represents a single oocyte tracked through meiotic progression that was determined to be aneuploid at MII.

In the presence of 0.04 μg/ml nocodazole, the majority of young and old oocytes arrested at MI when examined 13–14 h after meiotic resumption (Fig. 6, A and B). In contrast, about 70% of young and old oocytes that were cultured in DMSO as a control reached MII as indicated by PBE (Fig. 6, A and B). Four hours after the removal of nocodazole from the culture medium, greater than 80% of both young and old oocytes had resumed meiosis and emitted a PB, indicating that cell viability was not compromised by the drug treatment (Fig. 6, A and B). The incidence of aneuploidy, however, in the young and old eggs following drug removal was 60% (n = 15) and 67% (n = 20), respectively. These gross chromosome segregation defects are likely due to extended culture in an MI arrest and nonreversible effects of nocodazole, and indicate that the cell division machinery is compromised independent of maternal age. Overall these data suggest that, in response to a low concentration of spindle poison, young and old oocytes are able to activate the checkpoint to similar degrees.

DISCUSSION

Conventional genetic approaches that completely abrogate SAC function lead to severe phenotypes such as embryonic lethality and infertility [32–34]. Less severe disruption of the SAC, as occurs with the loss of one *Mad2* allele, results in meiosis I defects [12]. *Mad2*+/– oocytes have an accelerated AI onset, chromosome mis-segregation at meiosis I, and a 22.5% incidence of aneuploidy in the resulting eggs. Using a model of natural reproductive aging, we find that although old eggs have an incidence of aneuploidy comparable to that of *Mad2* heterozygotes, they do not undergo AI prematurely. Instead, old oocytes either have a longer average meiosis I duration or fail to progress to MII compared to young oocytes. Furthermore, old oocytes arrest at MI as well as young oocytes when exposed to a low concentration of nocodazole, indicating that old oocytes do possess an effective SAC. Measurements on populations of oocytes might miss a defective SAC in the

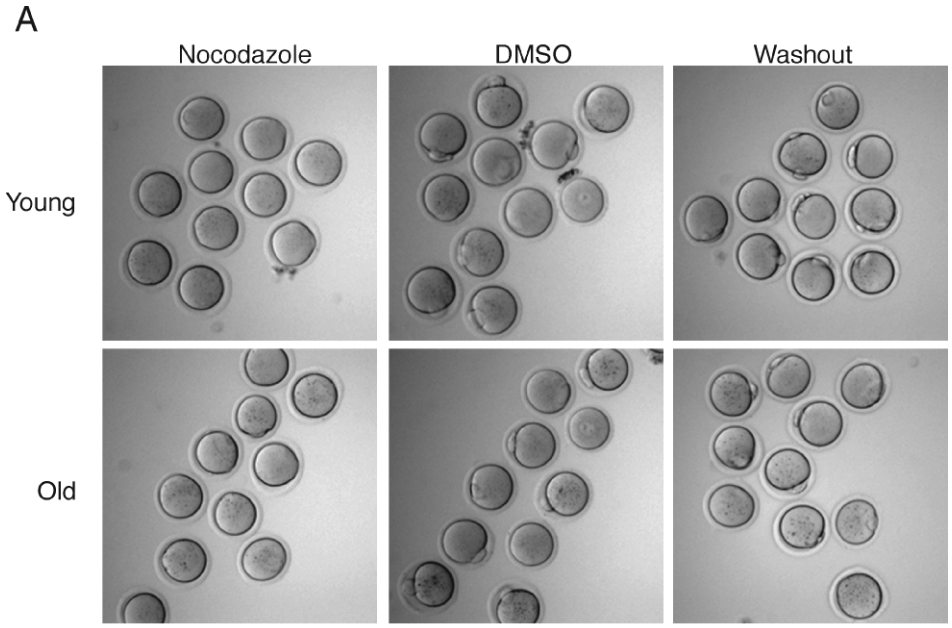

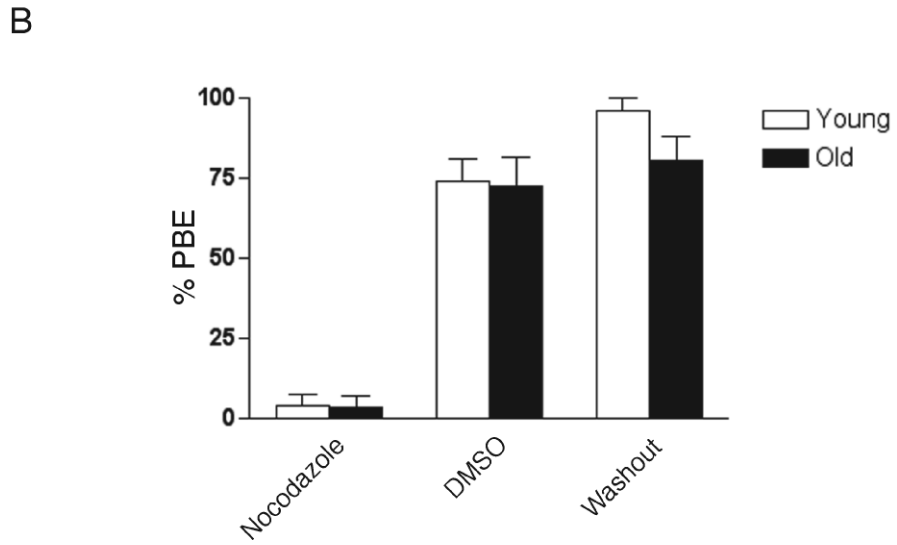

FIG. 6. Response of young and old oocytes to a low concentration of nocodazole. **A**) Representative morphology of young (top) and old (bottom) oocytes that were matured for 13–14 h in the presence of 0.04 μg/ml nocodazole (left) or in DMSO (middle) as a control. Following maturation, nocodazole was washed out of the medium, and the oocytes were scored 4 h later for PBE (right). Note the absence of PBs in young and old oocytes treated with nocodazole compared to controls, indicating SAC activation at meiosis I. **B**) Percent of oocytes from young and old mice that emitted a PB after being matured for 13–14 h in nocodazole or DMSO or after 4 h following washout of nocodazole. This experiment was repeated three times, and >30 young and old oocytes were analyzed in each treatment group. Data in the graph are expressed as the mean ± SEM. There were no statistically significant differences between young and old oocytes in each of the three treatment groups (two-way ANOVA; $P = 0.2733$).

subset of old oocytes that ultimately accounts for the ~30% aneuploidy incidence. Therefore, we analyzed timing of meiotic events in individual oocytes. If the SAC were defective in some old oocytes, we would expect a correlation between shorter meiosis I duration and aneuploidy, which was not observed. Taken together, these data suggest that a loss of SAC function is unlikely the primary cause of the maternal age-associated increase in aneuploidy.

Our results showing that the SAC is functional in both young and old oocytes contrasts with those reported using the CBA/Ca mouse strain [35], which is characterized by a limited follicle pool, a short reproductive span, and a maternal age-associated increase in egg aneuploidy [35, 36]. In oocytes from 9- to 10-mo-old CBA/Ca mice, the duration of meiosis I was 1.5 h less than in oocytes from 2- to 4-mo-old counterparts [35], in contrast to our results. However, this study was done without synchronizing meiotic resumption, and meiotic progression was monitored in cohorts of oocytes instead of in individuals. Furthermore, because the etiology of premature reproductive aging in CBA/Ca mice is unknown, this model may not be suitable for addressing the mechanisms of natural aging.

Although we used a natural reproductive aging mouse model, our system may not fully recapitulate meiotic maturation in vivo. For example, young and old mice were administered exogenous gonadotropin to stimulate follicle growth, and oocytes were matured in vitro in the absence of companion cumulus or granulosa cells. Nevertheless, young and old oocytes were treated the same, and the aneuploidy levels we report are consistent with those obtained from in vivo-matured MII eggs in this strain, for which hyperploidy was 4% in young oocytes and 25% in old oocytes [19]. Therefore, our results are likely to reflect maturation in vivo with respect to causes of aneuploidy.

Our findings indicate that SAC deterioration is not the primary cause of aneuploidy. However, we cannot exclude the possibility that subtle defects in SAC function might contribute to aneuploidy by unmasking other meiotic problems, such as in spindle assembly, kinetochore function, or cohesion. For example, kinetochore defects that interfere with microtubule binding would lead to chromosome segregation errors only if not detected by the SAC. Chromosome-specific factors also likely influence aneuploidy susceptibility because individual

chromosomes behave differently with respect to maternal age [37, 38]. These observations suggest that there may be multiple pathways leading to aneuploidy. An important future goal is to test whether other meiotic processes are compromised with age, to determine the primary causes of age-related aneuploidy. Our finding that the overall aneuploidy rate does not arise from an individual mouse suggests that reproductive aging is likely due to a general deterioration of a cellular process(es) that occurs in all animals and occasionally passes a threshold that leads to an error in chromosome segregation. Current studies are examining whether age-dependent changes in cohesion or kinetochore function contribute to the increased incidence of aneuploidy.

ACKNOWLEDGMENTS

We thank Karen Schindler for technical advice and for critically reading the manuscript and Hua Pan for generating the *H2b-Gfp* construct used in Figure 2D.

REFERENCES

1. Hassold T, Hunt P. To err (meiotically) is human: the genesis of human aneuploidy. Nat Rev Genet 2001; 2:280–291.
2. Pellestor F, Anahory T, Hamamah S. Effect of maternal age on the frequency of cytogenetic abnormalities in human oocytes. Cytogenet Genome Res 2005; 111:206–212.
3. Hassold T, Chiu D. Maternal age-specific rates of numerical chromosome abnormalities with special reference to trisomy. Hum Genet 1985; 70:11–17.
4. Warren W, Gorringe K. A molecular model for sporadic human aneuploidy. Trends Genet 2006; 22:218–224.
5. Jones KT. Meiosis in oocytes: predisposition to aneuploidy and its increased incidence with age. Hum Reprod Update 2008; 14:143–158.
6. Vogt E, Kirsch-Volders M, Parry J, Eichenlaub-Ritter U. Spindle formation, chromosome segregation and the spindle checkpoint in mammalian oocytes and susceptibility to meiotic error. Mutat Res 2008; 651:14–29.
7. Malmanche N, Maia A, Sunkel C. The spindle assembly checkpoint: preventing chromosome mis-segregation during mitosis and meiosis. FEBS Lett 2006; 580:2888–2895.
8. Musacchio A, Hardwick KG. The spindle checkpoint: structural insights into dynamic signalling. Nat Rev Mol Cell Biol 2002; 3:731–741.
9. Taylor SS, Scott MI, Holland AJ. The spindle checkpoint: a quality control mechanism which ensures accurate chromosome segregation. Chromosome Res 2004; 12:599–616.
10. Wassmann K, Niault T, Maro B. Metaphase I arrest upon activation of the Mad2-dependent spindle checkpoint in mouse oocytes. Curr Biol 2003; 13:1596–1608.
11. Homer HA, McDougall A, Levasseur M, Murdoch AP, Herbert M. Mad2 is required for inhibiting securin and cyclin B degradation following spindle depolymerisation in meiosis I mouse oocytes. Reproduction 2005; 130:829–843.
12. Niault T, Hached K, Sotillo R, Sorger PK, Maro B, Benezra R, Wassmann K. Changing Mad2 levels affects chromosome segregation and spindle assembly checkpoint control in female mouse meiosis I. PLoS ONE 2007; 2:e1165.
13. Homer HA, McDougall A, Levasseur M, Yallop K, Murdoch AP, Herbert M. Mad2 prevents aneuploidy and premature proteolysis of cyclin B and securin during meiosis I in mouse oocytes. Genes Dev 2005; 19:202–207.
14. Wang JY, Lei ZL, Nan CL, Yin S, Liu J, Hou Y, Li YL, Chen DY, Sun QY. RNA interference as a tool to study the function of MAD2 in mouse oocyte meiotic maturation. Mol Reprod Dev 2007; 74:116–124.
15. Tsurumi C, Hoffmann S, Geley S, Graeser R, Polanski Z. The spindle assembly checkpoint is not essential for CSF arrest of mouse oocytes. J Cell Biol 2004; 167:1037–1050.
16. Madgwick S, Jones KT. How eggs arrest at metaphase II: MPF stabilisation plus APC/C inhibition equals Cytostatic Factor. Cell division 2007; 2:4.
17. Miyamoto H, Manabe N, Mitani Y, Sugimoto N, Watanabe T, Aruga C, Sato E. Female reproductive properties and prenatal development of a senescence-accelerated mouse strain. J Exp Zool 1995; 272:116–122.
18. Liu L, Keefe DL. Ageing-associated aberration in meiosis of oocytes from senescence-accelerated mice. Hum Reprod 2002; 17:2678–2685.
19. Pan H, Ma P, Zhu W, Schultz R. Age-associated increase in aneuploidy and changes in gene expression in mouse eggs. Dev Biol 2008; 316:397–407.
20. Mori A, Utsumi K, Liu J, Hosokawa M. Oxidative damage in the senescence-accelerated mouse. Ann N Y Acad Sci 1998; 854:239–250.
21. Nakahara H, Kanno T, Inai Y, Utsumi K, Hiramatsu M, Mori A, Packer L. Mitochondrial dysfunction in the senescence accelerated mouse (SAM). Free Radic Biol Med 1998; 24:85–92.
22. Whitten WK. Nutrient requirements for the culture of preimplantation mouse embryos in vitro. Adv Biosci 1971; 6:129–139.
23. Chatot CL, Ziomek CA, Bavister BD, Lewis JL, Torres I. An improved culture medium supports development of random-bred 1-cell mouse embryos in vitro. J Reprod Fertil 1989; 86:679–688.
24. Duncan FE, Moss SB, Schultz RM, Williams CJ. PAR–3 defines a central subdomain of the cortical actin cap in mouse eggs. Dev Biol 2005; 280: 38–47.
25. Tsafriri A, Chun SY, Zhang R, Hsueh AJ, Conti M. Oocyte maturation involves compartmentalization and opposing changes of cAMP levels in follicular somatic and germ cells: studies using selective phosphodiesterase inhibitors. Dev Biol 1996; 178:393–402.
26. Mayer TU, Kapoor TM, Haggarty SJ, King RW, Schreiber SL, Mitchison TJ. Small molecule inhibitor of mitotic spindle bipolarity identified in a phenotype-based screen. Science 1999; 286:971–974.
27. Kozak M. At least six nucleotides preceding the AUG initiator codon enhance translation in mammalian cells. J Mol Biol 1987; 196:947–950.
28. Igarashi H, Knott JG, Schultz RM, Williams CJ. Alterations of PLCbeta1 in mouse eggs change calcium oscillatory behavior following fertilization. Dev Biol 2007; 312:321–330.
29. Xiong B, Li S, Ai JS, Yin S, Ouyang YC, Sun SC, Chen DY, Sun QY. BRCA1 is required for meiotic spindle assembly and spindle assembly checkpoint activation in mouse oocytes. Biol Reprod 2008; 79:718–726.
30. Tarkowski AK. An air-drying method for chromosome preparations from mouse eggs. Cytogenetics 1966; 5:394–400.
31. Hodges C, Hunt P. Simultaneous analysis of chromosomes and chromosome-associated proteins in mammalian oocytes and embryos. Chromosoma 2002; 111:165–169.
32. Kalitsis P, Earle E, Fowler KJ, Choo KH. Bub3 gene disruption in mice reveals essential mitotic spindle checkpoint function during early embryogenesis. Genes Dev 2000; 14:2277–2282.
33. Dobles M, Liberal V, Scott ML, Benezra R, Sorger PK. Chromosome missegregation and apoptosis in mice lacking the mitotic checkpoint protein Mad2. Cell 2000; 101:635–645.
34. Baker DJ, Jeganathan KB, Cameron JD, Thompson M, Juneja S, Kopecka A, Kumar R, Jenkins RB, de Groen PC, Roche P, van Deursen JM. BubR1 insufficiency causes early onset of aging-associated phenotypes and infertility in mice. Nat Genet 2004; 36:744–749.
35. Eichenlaub-Ritter U, Boll I. Age-related non-disjunction, spindle formation and progression through maturation of mammalian oocytes. Prog Clin Biol Res 1989; 318:259–269.
36. Eichenlaub-Ritter U. Genetics of oocyte ageing. Maturitas 1998; 30:143–169.
37. Nicolaidis P, Petersen MB. Origin and mechanisms of non-disjunction in human autosomal trisomies. Hum Reprod 1998; 13:313–319.
38. Warburton D, Kinney A. Chromosomal differences in susceptibility to meiotic aneuploidy. Environ Mol Mutagen 1996; 28:237–247.